Cement & Concrete Composites 34 (2012) 739–745

Contents lists available at SciVerse ScienceDirect

Cement & Concrete Composites

journal homepage: www.elsevier.com/locate/cemconcomp

Identification of the percolation threshold in cementitious pastes by monitoring the *E*-modulus evolution

Lino Maia [a,b,*], Miguel Azenha [c], Rui Faria [a], Joaquim Figueiras [a]

[a] LABEST – Laboratory for the Concrete Technology and Structural Behaviour, Faculdade de Engenharia, Universidade do Porto, Rua Dr. Roberto Frias, 4200-465 Porto, Portugal
[b] Centro de Ciências Exatas e da Engenharia, Universidade da Madeira, Campus Universitário da Penteada, 9020-105 Funchal, Portugal
[c] ISISE – Institute for Sustainability and Innovation in Structural Engineering, Universidade do Minho, Escola de Engenharia, Campus de Azurém, 4800-058 Guimarães, Portugal

ARTICLE INFO

Article history:
Received 14 March 2011
Received in revised form 1 March 2012
Accepted 2 March 2012
Available online 9 March 2012

Keywords:
Cementitious pastes
Percolation threshold
Ambient vibration method
Early ages

ABSTRACT

The determination of the fluid-to-solid transition in cement-based materials is fundamental to understanding the evolution of early-age mechanical properties and to detect the time after which the material may withstand stresses. The transition is gradual, and non-destructive methods are needed for clear identification. This paper presents a study using a recent method for continuously monitoring the *E*-modulus of cement-based materials since casting, based on evaluating the first resonant frequency of a composite beam containing the material under test. It is intended to demonstrate the capability of this method to detect the percolation threshold and to check eventual correlations with the released heat of hydration. Five sets of mix compositions are tested, with w/c ratios ranging from 0.30 to 0.50, with the addition of limestone filler, or with partial replacement of cement by fly ash, silica fume or metakaolin.

1. Introduction

Cement-based materials endure volume changes during hydration and beyond, which upon restraint may cause tensile stresses to develop, leading to non-negligible cracking risks on structures. These changes are due to thermal and moisture variations [1], caused by external and autogenous conditions. Of particular relevance for the latter, hydration reactions play a fundamental role at early-ages, when the rates of water consumption and of released heat are important, and the tensile strength of the hardening material is low. Thus, identification of the early-age transition from fluid-to-solid of a cement-based material, and awareness of the time when its particles become connected due to the growth of hydration products – the percolation threshold –, are crucial issues towards predicting early-age stresses and evaluating cracking risks.

The Vicat Needle [2] and the Proctor Penetration Resistance [3] tests are widely used to assess the setting time. However, they cannot describe precisely the fluid-to-solid transition, as their measurements indicate only when the microstructure has already reached a minimum of penetration or shear resistance. Accordingly, they do not provide a truly mechanical identification in regards to the percolated particles network, because the setting time is registered with a delay [4,5]. Furthermore, these tests provide discontinuous measurements, and considering that the fluid-to-solid transition is gradual, non-destructive but continuous measurements are preferable [6].

Taking advantage of the continuous nature of measurements from calorimetric methods, some researchers [7–10] estimate the setting time through the released heat of cement hydration, even though the released heat of cement hydration is not directly related to the percolated network evolution [5,11]. An example of such calorimetric approaches can be found in Wang et al. [7], who used a semi-adiabatic calorimeter and reported linear correlations between the maximum derivate of the temperature-time curve and the initial setting defined in ASTM C403 [3].

Combining rheometric with ultrasonic [12] or calorimetric [13] methods, the viscoelastic behaviour of cement pastes at very early ages has also been monitored. The authors reported that the storage shear modulus (which is closely related to the volume fraction of solid particles) remains at approximately 0.01 GPa up to the end of the dormant period. From then on the storage modulus increases much more than the loss modulus, which indicates that the elastic properties of the material become measurable, i.e., the fluid-to-solid transition was surpassed. Even though rheometric methods clearly describe the fluid-to-solid transition, they are unsuitable to describe the *E*-modulus evolution in hardening materials after setting.

Through the measurement of mechanical properties of the hardening material, such as the *E*-modulus or the compressive strength, the development of the percolated network can be directly evaluated [14]. However, at the onset of the solid network

* Corresponding author. Address: LABEST – Laboratory for the Concrete Technology and Structural Behaviour, Faculdade de Engenharia, Universidade do Porto, Rua Dr. Roberto Frias, 4200-465 Porto, Portugal. Tel.: +351 966096541; fax: +351 225081835.
E-mail addresses: lino.maia@fe.up.pt (L. Maia), miguel.azenha@civil.uminho.pt (M. Azenha), rfaria@fe.up.pt (R. Faria), jafig@fe.up.pt (J. Figueiras).

0958-9465/$ - see front matter © 2012 Elsevier Ltd. All rights reserved.
http://dx.doi.org/10.1016/j.cemconcomp.2012.03.001

formation it is difficult to assess these properties, so indirect methods are needed. For example, methods based on resonant frequency techniques [15] were used in [16–18], although with techniques mostly devised for concrete. Since the 1990s ultrasonic methods have been widely adopted to identify the setting, as well as to monitor the early-age hardening of pastes, mortars and concretes [19–29]. However, ultrasonic methods partially fail when material homogeneity is lacking (such as in plastic pastes not deaired, wherein compressional waves do not propagate properly [11]), and when shear waves are applied in a medium that is still fluid [30].

Recently Azenha et al. [31] proposed a novel method to measure the *E*-modulus evolution in concrete, called 'Elasticity Modulus Monitoring through Ambient Response Method' (EMM-ARM), which is based on the evolution of the natural frequency of vibration of a composite beam, filled with the material under testing. The method allows continuous measurements immediately after casting, and was used also to identify the *E*-modulus evolution of cement pastes with different admixtures or different additions [32,33]. The authors reported that the EMM-ARM was able to detect the effect of admixture retarders/accelerators or mineral/cementitious additions on the *E*-modulus evolution. However, so far the capability of the method to describe the fluid-to-solid transition was neither explored, nor tested.

In the present paper the potential of the EMM-ARM to describe the fluid-to-solid transition in cementitious pastes, as well as to identify the percolation threshold, will be assessed. The evolution curves of the *E*-modulus (assessed by the EMM-ARM) and of the released heat of hydration (measured via an isothermal calorimeter) will be compared at early ages. Furthermore, the power law suggested in the percolation theory [34] will be fitted to the *E*-modulus curve, so as to identify the percolation threshold. Results concerning the fluid-to-solid transition on 17 cementitious pastes will be presented, involving mixes where the following characteristics were varied, to cover a wide range of situations: (i) the water-to-cement (w/c) ratio, (ii) the limestone filler content, and the use of (iii) fly ash, (iv) silica fume and (v) metakaolin as partial replacements of cement.

2. Theory and methods

2.1. The EMM-ARM

In the EMM-ARM the natural frequency of vibration of a composite cantilever – formed by an acrylic tube filled with the paste under testing (see Fig. 1) – is related to the *E*-modulus of the cementitious material, using expressions well established in structural modal identification. Generally speaking, as an increase of the *E*-modulus of the cementitious material enforces a concomitant growth on the structural stiffness of the composite cantilever, the flexural frequency of vibration of the latter rises during cement hydration, whilst the suspension gradually evolves into an elastic solid. During the suspension period the stiffness of the cementitious material is negligible, although not its mass, but the method still applies because the acrylic tube is stiff enough to allow frequency measurements to be made on the cantilever. Along the experiment the frequency identification is made via continuous measurements of the vertical accelerations induced on the free extremity of the cantilever by ambient vibration (associated to wind or mechanical ventilation, traffic, working machinery, etc.), made with a small accelerometer. So, the experiment is completely autonomous and non-destructive, thus suitable to undertake the continuous identification of the *E*-modulus of pastes since casting.

The natural frequency of the cantilever experiences a remarkable increase upon formation of the percolated solid network at the percolation threshold, which may be used to indicate the onset of material structure formation and development of elastic properties. According to this proposal, identification of the percolation threshold can be based on the natural frequency change observed on the cantilever, and concomitantly on the related change on the *E*-modulus of the cementitious material, identified by the EMM-ARM.

The EMM-ARM methodology used for the present work has been detailed elsewhere [32], so its description will be limited to just essential aspects concerning the setup geometry, experimental procedure and data acquisition and treatment. The overall geometry of the test setup is reproduced in Fig. 1: it consists of a 600 mm long acrylic tube, with internal and external diameters of $\phi_i = 16$ mm and $\phi_e = 20$ mm, into which the cement paste is cast. The resulting beam (acrylic tube and cement paste) is then placed horizontally and clamped with recourse to steel devices (see Fig. 1b), forming a cantilever with a 450 mm free span (see Fig. 1a). At the cantilever's right extremity the acrylic tube lid is prepared with a nut, onto which a lightweight accelerometer is fixed, as shown in Fig. 1c and d. From the beginning of the casting operations (undertaken with the acrylic tube standing upright, filled through the left extremity shown in Fig. 1a), and until the onset of acceleration measurements with the composite cantilever duly supported and placed horizontally, approximately 25 min are spent.

The modal identification technique that is adopted to identify the flexural frequency of vibration of the composite cantilever belongs to a category known as "output-only" [35,36], and it relies on the assumption that the vibrations of the environment

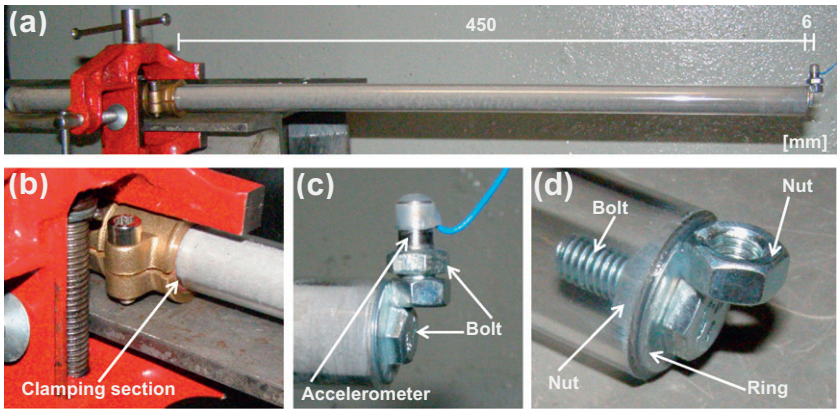

Fig. 1. (a) Experimental setup in the measuring position for the EMM-ARM; (b) clamping section; (c) accelerometer detail; (d) free extremity.

surrounding the tested beam (i.e., the ambient vibrations) occur on average as a white noise, with a uniform energy content throughout the range of frequencies of interest. In terms of accelerations (e.g., along the vertical direction), the response of a structure under this ambient loading has amplitude peaks in resonance with their natural frequencies of vibration.

The overall process pursued to identify the first flexural resonant frequency of the cantilever is outlined on the flow diagram depicted in Fig. 2. The electric signal generated by the accelerometer placed at the cantilever free extremity is amplified and continuously fed into a data logger at a 200 Hz frequency (more than twice the maximum expectable resonant frequency of the first flexural mode of vibration), which in turn is stored in a computer (after the transformation of the voltage into acceleration values). The information is then cropped into packets of 15 min of duration, each of them being handled separately in MATLAB to identify the average resonant frequency of the beam in that period. Each data packet is treated according to the Welch procedure [37]: (i) the data packet is separated into sub-packets (each containing 4096 points), with 50% data overlapping; (ii) Hanning windows are applied to each sub-packet, and FFT (Fast Fourier Transform) algorithms are used to obtain power spectra; (iii) the power spectra of the sub-packets are then normalized and averaged, leading to the averaged normalized power spectrum of each packet of 15 min duration. Three examples of the computed power spectra are shown in Fig. 2 for the instants of $t = 1.5$ h, $t = 10$ h and $t = 36$ h: it can be confirmed that during time the response peak is shifting from lower to higher frequencies, as a consequence of cement hydration. If all computed power spectra are put side-by-side according to their time of occurrence, a meaningful colour map may be obtained, in which the intensity of the signal is proportional to a colour scale as shown in Fig. 2. Interpretation of such a colour map is quite intuitive, and the continuous trend of evolution of the resonant frequency is clearly identified. By tracking the peak frequency along time on the colour map, it is possible to plot the resonant frequency of the cantilever along time, as also illustrated in Fig. 2.

The last step of application of the EMM-ARM consists in using the dynamic equation of motion of the composite cantilever [38]:

$$a^3[\cosh(aL)\cos(aL)-1] = \frac{-w^2M}{EI}[\cos(aL)\sinh(aL)-\cosh(aL)\sin(aL)] \quad \text{with } a = \sqrt[4]{\frac{w^2m}{EI}} \tag{1}$$

where $w = 2\pi f$ (with f being the natural frequency of vibration), L is the free span, m is the uniformly distributed mass (owing to the acrylic tube and the mix), M is the concentrated mass at the free extremity (owing to the accelerometer, nuts, bolts and closing lid – see Fig. 1c and d), and E is the E-modulus and I is the second moment of area of the composite beam. Therefore, for each measured frequency f it is possible to estimate the corresponding EI of the composite cantilever, and given the fact that the E-modulus of acrylic E_a is known, it is possible to obtain the E-modulus of the paste E_p as

$$E_p = EI\frac{64}{\pi\phi_i^4} - E_a\frac{\phi_e^4-\phi_i^4}{\phi_i^4} \tag{2}$$

The whole set of operations that has been described for modal identification and E-modulus computation is imperceptible to the final user, who rather easily gets the evolutive E-modulus curve along cement hydration for each experiment.

2.2. Percolation theory

Another possibility to identify the fluid-to-solid transition in cementitious pastes may be based on the percolation theory [30,39]. At very early ages the hydrates around the cement grains initiate the development of small clusters, which turn into bigger ones with the consequent increase of the degree of connectivity. Bentz and Garboczi [39], who developed a microstructural model to describe the percolation or connectivity of the phases as a function of hydration, provided a detailed explanation concerning the application of the percolation theory in the cement hydration context. Defining by p the average degree of connectivity, the percolation threshold p_c is reached when the interconnected solid network is fully developed throughout the whole material. Near the percolation threshold the macroscopic conductance Σ follows a power law [34] of the form

$$\Sigma = A(p-p_c)^{\mu} \tag{3}$$

where A is a constant and μ is the critical exponent of the percolation problem.

Many other physical properties evolve along cement hydration analogously to Σ, and E_p is one of them. In that case Eq. (3) may assume the form

$$E_p = E_0(p-p_c)^{\mu_0} \tag{4}$$

where E_0 and μ_0 are the material constants for the actual property. Considering that the number of contacts between the clinker particles increases in time t according to a power law (as assumed in [40]), in the neighbourhood of the critical time t_c the evolution of E_p may be expressed as a function of time according to

$$E_p = E_0'(t-t_c)^{\mu_0'} \tag{5}$$

where E_0' and μ_0' are material constants. By minimizing the sum of square differences between the experimentally identified values of E_p and the ones obtained analytically when different sets of E_0', μ_0' and t_c are tested in Eq. (5), the most suitable value of t_c may finally be determined.

2.3. Calorimetry

As the released heat during cement hydration is a physical property related to the chemical reactions of cement-based materials [4,5,7,13,19], calorimetric measurements are sometimes used to provide indications of the physical setting time [7–10]. In fact, although from a material's science perspective heat generation and setting time are not strictly related, at the end of the dormant period the increasing of hydration is so dramatic that in engineering practice the rate of change of the released heat is often used for that purpose [5,11]. For the present research an isothermal conduction calorimeter (JAF60) was used, its measurements being compared to the conclusions of EMM-ARM, as far as the percolation threshold time identification is concerned. Further details about this kind of equipment and its measuring principles can be found in [41].

3. Experimental program

3.1. Materials and mix compositions

In the present research an experimental program was conducted to determine the percolation threshold in pastes. The materials used for the mixes were obtained on the Portuguese market, which included: CEM I 42.5R cement (c) according to EN 197-1 [42], limestone filler (f), fly ash (fa), silica fume (sf), metakaolin (mtk) and distilled water (w). Seventeen mixes were prepared

Table 1
Mix compositions of the pastes used.

Mix	Name	c (g)	f (g)	fa (g)	sf (g)	mtk (g)	w (g)
1	w/c = 0.30	320					96
2	w/c = 0.35	320					112
3	w/c = 0.40	320					128
4	w/c = 0.45	320					144
5	w/c = 0.50	320					160
6	f/c = 0.15	320	48				144
7	f/c = 0.30	320	96				144
8	f/c = 0.45	320	144				144
9	fa/b = 0.20	256		64			144
10	fa/b = 0.40	192		128			144
11	fa/b = 0.60	128		192			144
12	sf/b = 0.05	304			16		144
13	sf/b = 0.10	288			32		144
14	sf/b = 0.15	272			48		144
15	mtk/b = 0.05	304				16	144
16	mtk/b = 0.10	288				32	144
17	mtk/b = 0.15	272				48	144

using 320 g of binder (b) in each, all other mix contents being weighed according to the ratios specified in Table 1. Limestone filler was considered solely as powder, whereas fly ash, silica fume and metakaolin were considered as binders. Mix 4, with w/c = 0.45 and f/c = fa/b = sf/b = mtk/b = 0, should be considered the reference one.

Mixes were prepared in plastic containers using a mixer with a vertical paddle, according to the following procedure: (i) water was added to the powders (which defines the measuring start time, $t = 0$), (ii) mixing started at a speed of 500 rpm, extending for 3 min, (iii) mixing stopped for 2 min, and (iv) mixing resumed at a speed of 2000 rpm for 2 min. All mixes were made twice, one for the EMM-ARM test and other for the isothermal calorimeter.

3.2. Pouring and testing for the EMM-ARM

In regards to the preparation of the composite cantilever used in the EMM-ARM tests, immediately after mixing the acrylic tube (with one extremity closed with a ring and a bolt – see Fig. 1d) was used as a mould, and filled up with paste. Upon completion of the filling, the tube was carefully vibrated to expel air bubbles, and then hot glue (which cools down and hardens within seconds) was used to close the other extremity of the mould. Approximately 20 min after '$t = 0$' the acrylic tube filled with the paste was fixed at the measuring position, and an accelerometer was screwed on the free end of the cantilever. The first measurements of vertical accelerations started 25 min after '$t = 0$'; subsequent measurements were performed continuously, at least up to the age of 12 h. The tests were carried out inside a climatic chamber, with controlled temperature at 20.0 ± 0.3 °C.

One sample per mix was tested, but to assess repeatability of the EMM-ARM procedure mixes 4 and 7 were performed twice. Similar *E*-modulus evolutions for each pair of mixes were found, with the maximum difference obtained during the first 12 h being under 0.3 GPa. In order to control maturity, the temperature was measured inside the cement paste. As a result, it was observed that the temperature did not vary more than ±1 °C (the maximum variation took place for the mix 1), thus maturity corrections were considered unnecessary.

3.3. Pouring and testing for the calorimetry

For characterization in the isothermal calorimeter, after mixing each paste was poured inside a plastic bag, thereafter carefully sealed through thermo-welding. All pastes were studied using samples containing exactly 30 g of binder, with their total weights satisfying the mix proportions indicated in Table 1. Two samples were analyzed per mix, and the results presented in this paper correspond to the average of each pair. The testing temperature was constant, with a value of 20 °C throughout the whole experiment.

4. Test results and discussion

4.1. Resolution of the EMM-ARM

The EMM-ARM allows for the determination of the paste E-moduli every 15 min, but due to the fact that the resolution of

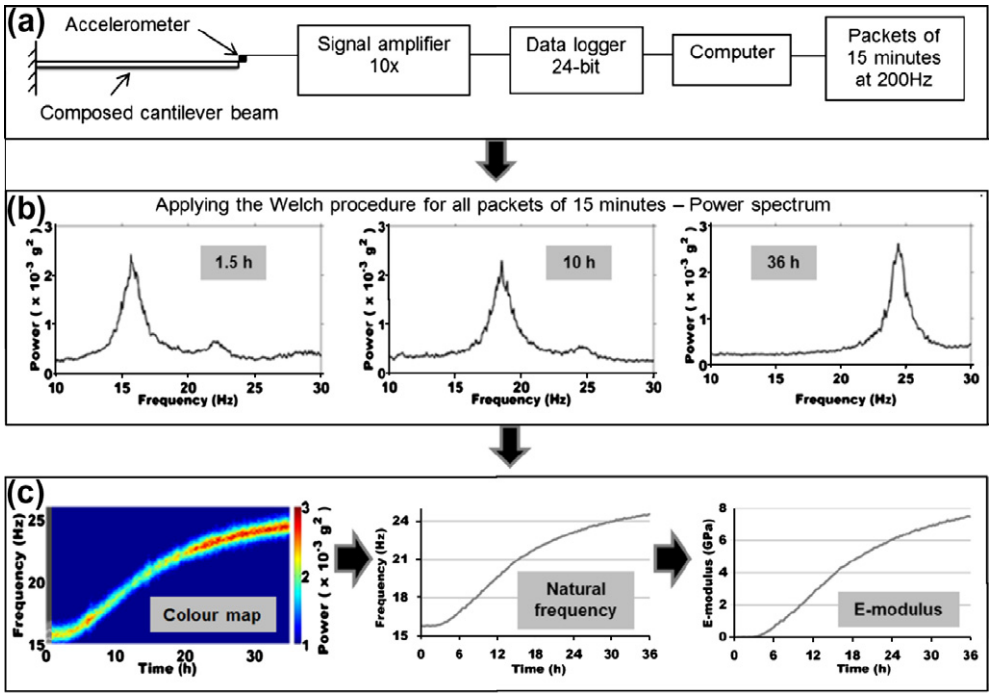

Fig. 2. Schematic setup and data processing: (a) data reading, (b) power spectrum, and (c) *E*-modulus evolution.

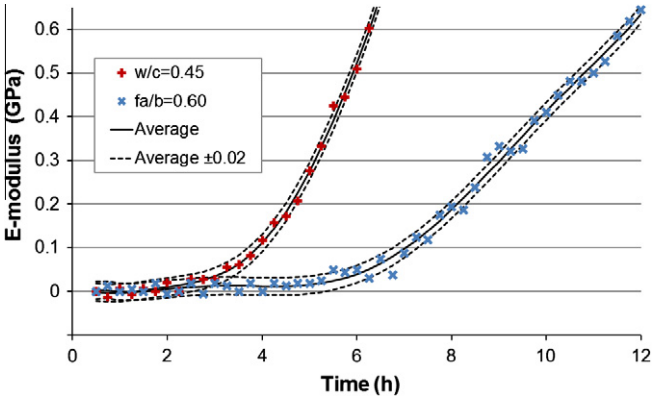

Fig. 3. Resolution of the EMM-ARM on measurements of the paste *E*-modulus.

the method is limited, the trend line that is obtained exhibits some slight oscillations. Looking at Fig. 3, where the very early age outcomes from the EMM-ARM are reported for two mixes, it is possible to observe that before setting the E-moduli are not exactly zero. Thus, in order to investigate the ability of the EMM-ARM to describe the fluid-to-solid transition and to identify the percolation threshold, the resolution of the method will be checked out first.

In regard to the E-moduli reported in Fig. 3 (note that similar findings were obtained for the other mixes studied), it can be observed that approximately 90% of the values fall within a range of ±0.02 GPa relative to an average trend line, the latter defined by fitting a six-degree polynomial. Thus, with a resolution of ±0.02 GPa the EMM-ARM is not an appropriate technique to study the viscosity evolution during the dormant period (as provided by rheometric methods) [20,43]. However, as the increase of the *E*-modulus is so dramatic immediately after the fluid-to-solid transition, the resolution of the EMM-ARM is considered adequate enough to detect the percolation threshold.

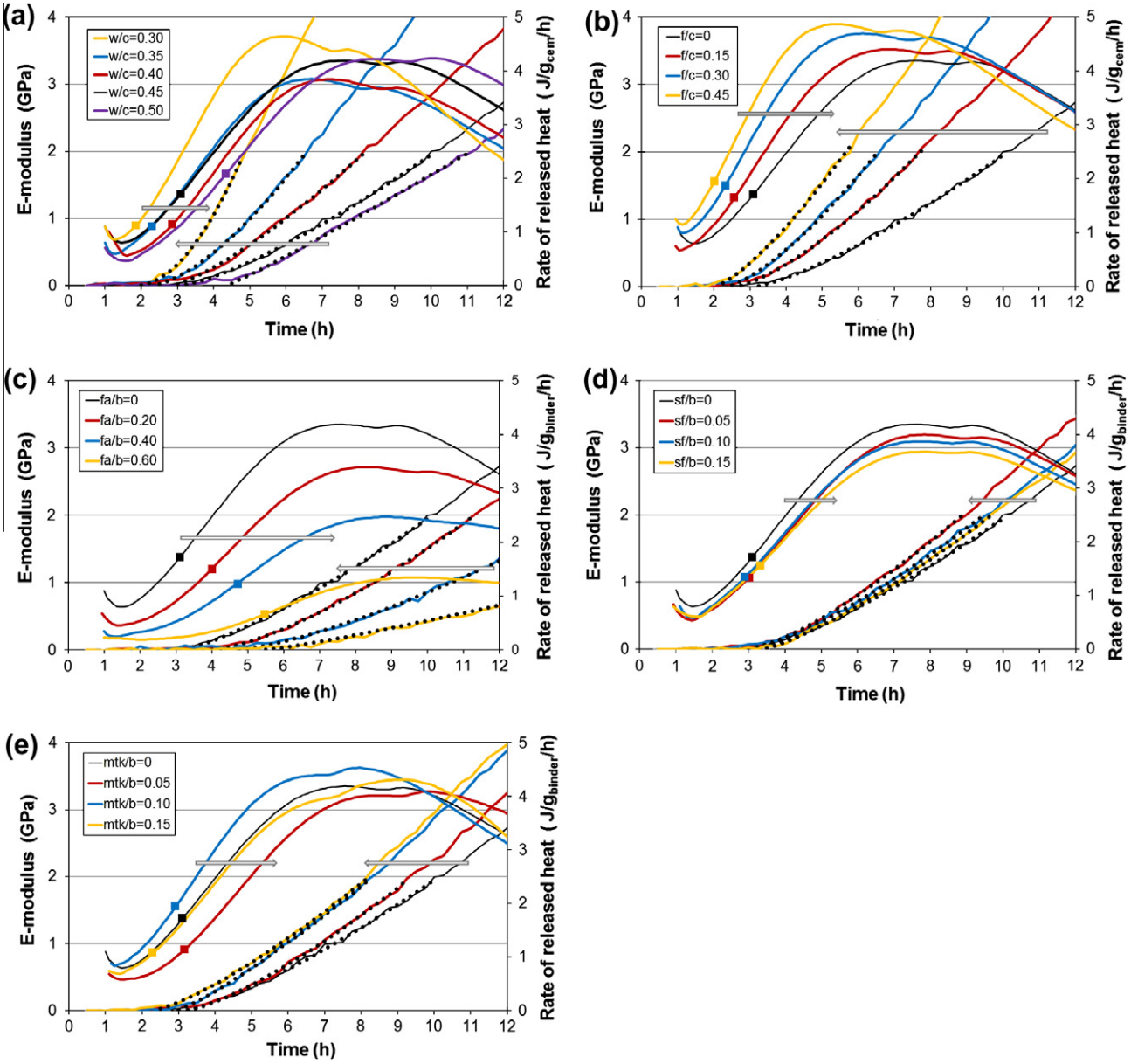

Fig. 4. Evolution curves for mixes with different ratios of: (a) w/c, (b) f/c (w/c = 0.45), (c) fa/b (w/b = 0.45), (d) sf/b (w/b = 0.45) and (e) mtk/b (w/b = 0.45) – dotted lines are power law fittings to the experimental results.

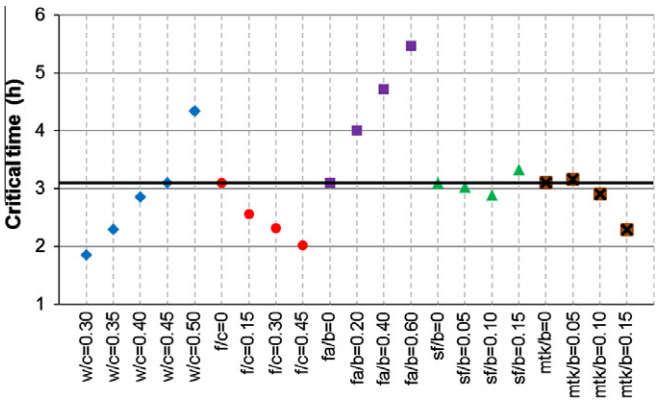

Fig. 5. Evolution of the percolation threshold.

4.2. Fluid-to-solid transition and identification of the percolation threshold

The E-moduli evolutions assessed through the EMM-ARM up to the age of 12 h are documented in Fig. 4 (note that w/c = 0.45, f/c = 0, fa/b = 0, sf/b = 0 and mtk/b = 0 are equivalent indications for the reference mix). Furthermore, the power laws fitted to the EMM-ARM results (as explained in Section 2.2) are also plotted in Fig. 4 as dotted lines, to allow identification of the percolation thresholds by calculating the critical times. Note that information available in the literature [30,34] does not define the extent of data that shall be considered near the percolation threshold. Upon analysis of several scenarios for this paper, values of E_p ranging within the interval 0.1-2.0 GPa were considered near the percolation threshold.

In the same graphs of Fig. 4 the rates of released heat of hydration obtained from isothermal calorimetry are reproduced as well (search for the curves crossed by the arrows pointing rightwards). In Fig. 4 over each curve concerning the rate of released heat of hydration a coloured square has been added, which corresponds to the instant at which the percolation threshold is identified for the same mix through the EMM-ARM data combined with the adjusted power law. This can help the assessment of possible relationships between rate of heat development and the percolation threshold.

Concerning the power laws proposed by the percolation theory, in Fig. 4 one observes that they describe appropriately the *E*-modulus evolution immediately after setting. Then, extending the power laws up to the axis of abscissas, the critical time is determined and used as the percolation threshold.

Analyzing Fig. 4 one can see that, as expected, the percolation threshold occurs always during the accelerating period of the hydration heat release [5,43]. In fact, after the end of the dormant period some hydration has to take place to provide the minimum solid assemblage required for the percolation threshold. Moreover, as previously mentioned by Dehadrai et al. [5], it is also observed that the percolation threshold does not correspond to any specific point on the rate of released heat of hydration curves.

In order to compare the obtained percolation thresholds detected in Fig. 4 with findings previously reported in the literature, Fig. 5 clarifies tendencies associated to mix compositions. For the set of mixes with different w/c ratios, Fig. 5 shows noticeably that the percolation threshold increases with the w/c, which actually corresponds to the growth of the clinker dilution effect. Moreover, Fig. 4a emphasises the strong influence of the w/c ratio on the evolution of the cement hydration: the greater the w/c, the lower the rate of increase of the *E*-modulus. Performing tests with ultrasonic methods several researchers [20,21,24,28–30] reported this tendency as well.

Well-defined tendencies are observed as well in Fig. 5 for the set of mixes containing limestone filler, with a clear reduction of the critical time as f/c increases. In Fig. 4b it was also observed that increasing f/c enhances the *E*-modulus and the early-age heat of hydration evolutions. These tendencies are explained by the shortening of the dormant period and the solid assemblage enhancement induced by the limestone filler, reported also in [44,45].

For the mixes where cement is partially replaced by additions, the effects of pozzolanic activity and of clinker dilution control the hydration [46,47]. According to the results reported in Fig. 4c and Fig. 5, the fly ash not only delays initiation of the *E*-modulus development, but also strongly lowers its evolution rate. Due to the effect of clinker dilution, similar tendencies are observed concerning the released heat of hydration. These findings are in agreement with the results reported in [48], where heat production rates and ultrasonic wave transmission measurements were compared in mortars with several fly ash contents.

As far as the silica fume addition is concerned, the dilution effect on the released heat of hydration is dominant on the results of Fig. 4d. This is similar to what is reported in [47], but different from results in [46,49] wherein the pozzolanic effect is dominant (probably due to different physical or chemical properties of the silica fume used). For the *E*-modulus evolution the percolation threshold is almost insensitive to the variations on the sf/b ratio (see Fig. 5), and in Fig. 4d one observes that after setting the higher *E*-modulus development occurs for sf/b = 0.05 (the lowest replacement).

Fig. 4e reports the influence of partial replacement of cement by metakaolin. No clear tendency is seen in terms of the released heat of hydration when mtk/b is changed. Snelson et al. [50] carried out calorimetric studies with metakaolin, and also reported findings without well-defined tendencies. Concerning the *E*-modulus evolution, Fig. 4e puts into evidence that it experiences a growth rate increase as the mtk/b ratios rises. Moreover, according to Fig. 5 it is observed that solely for the highest metakaolin content (mtk/b = 0.15) the percolation threshold time is significantly reduced.

5. Conclusions

In this paper the fluid-to-solid transition of several pastes during hydration was continuously monitored through measurements of the *E*-modulus, assessed by using a recent experimental method termed EMM-ARM. This method basically consists of monitoring the evolution of the first natural frequency of a small composite cantilever, formed by an acrylic cylindrical tube filled with the cementitious material under testing. At early ages the *E*-modulus evolution curve can be fitted by a power law, which allows the determination of the percolation threshold. The fluid-to-solid transition of 17 mixes was described by the EMM-ARM with an accuracy of ca. ±0.02 GPa.

The released heat of hydration was evaluated as well via an isothermal conduction calorimeter, to monitor the hydration reaction during the transition from fluid to solid. It was observed, as expected, that the percolation threshold occurs during the accelerating period of the rate of the released heat of hydration curve, and it does not coincide with any specific feature of this curve.

The EMM-ARM has sensibility to detect the percolation threshold variations due to paste composition changes, as well as to monitor the *E*-modulus evolution after the percolation threshold. Well-defined and consistent tendencies were observed for the studied mixes. The percolation threshold time increases with the w/c ratio and with the cement replacement by fly ash, and decreases when increasing the limestone filler content and decreasing the cement substitution by metakaolin. The EMM-ARM

showed also that the percolation threshold time remains practically unchanged when cement is replaced by silica fume.

Acknowledgments

Funding provided by the Portuguese Foundation for Science and Technology (FCT) and the European Social Fund (ESF), namely for the Research Projects PTDC/ECM/70693/2006 and PTDC/ECM/099250/2008, and to the first author through the PhD grant SFRH/BD/24427/2005, is gratefully acknowledged.

References

[1] ACI 231R-10. Report on Early-Age Cracking: Causes, Measurement, and Mitigation. Reported by ACI Committee 231: ACI; 2010.
[2] EN 196-3:2005, Methods of testing cement—Part 3: Determination of setting times and soundness, April 2005. 2005.
[3] ASTM C 403. Standard test method for time of setting of concrete mixtures by penetration resistance. American Society for Testing and Materials, Philadelphia, PA, 1985.
[4] Principallo A, Lura P, van Breugel K, Levita G. Early development of properties in a cement paste: a numerical and experimental study. Cem Concr Res 2003;33(7):1013–20.
[5] Dehadrai M, Sant G, Bentz D, Weiss J. Identifying the fluid-to-solid transition in cementitious materials at early ages using ultrasonic wave velocity and computer simulation. Concr Int 2009;259:66–76.
[6] Krauß M, Hariri K. Determination of initial degree of hydration for improvement of early-age properties of concrete using ultrasonic wave propagation. Cem Concr Compos 2006;28(4):299–306.
[7] Wang K, Ge Z, Grove J, Mauricio Ruiz J, Rasmussen R, Ferragut T. Developing a simple and rapid test for monitoring the heat evolution of concrete mixtures for both laboratory and field applications – Phase I. Center for Transportation Research and Education, Iowa State University; 2006.
[8] Schindler AK. Prediction of concrete setting. In: Weiss WJ, Kovler K, Marchand J, Mindess S, editor. Advances in concrete through science and engineering. In: RILEM Proceedings Pro 48, Proceedings of the 1st International RILEM, Symposium 2004.
[9] Schindler AK, Dossey T, McCullough BF. Temperature control during construction to improve the long term performance of portland cement concrete pavements. In: 0-1700-2 FHARRN, editor.: Center for Transportation Research, The University of Texas at Austin; 2002. p. 518.
[10] Wang K, Ge Z, Grove J, Mauricio Ruiz J, Rasmussen R, Ferragut T. Developing a simple and rapid test for monitoring the heat evolution of concrete mixtures for both laboratory and field applications – Phase II. Center for Transportation Research and Education, Iowa State University; 2007.
[11] Sant G, Dehadrai M, Bentz D, Lura P, Ferraris CF, Bullard JW, et al. Detecting the fluid-to-solid transition in cement pastes. Concr Int 2009;31(6):53–8.
[12] Sun Z, Voigt T, Shah SP. Rheometric and ultrasonic investigations of viscoelastic properties of fresh Portland cement pastes. Cem Concr Res 2006;36(2):278–87.
[13] Banfill PFG, Carter RE, Weaver PJ. Simultaneous rheological and kinetic measurements on cement pastes. Cem Concr Res 1991;21(6):1148–54.
[14] Bentz DP. A review of early-age properties of cement-based materials. Cem Concr Res 2008;38(2):196–204.
[15] ASTM C 215. Standard test method for fundamental transverse, longitudinal, and torsional resonant frequencies of concrete specimens. American Society for Testing and Materials, Philadelphia, PA, 2002.
[16] Pessiki SP, Carino NJ. Setting time and strength of concrete using the impact-echo method. ACI Mater J 1988;85(5):389–99.
[17] Nagy A. Determination of *E*-modulus of Young concrete with nondestructive method. J Mater Civil Eng 1997;9(1):15–20.
[18] Lee K-M, Kim D-S, Kim J-S. Determination of dynamic Young's modulus of concrete at early ages by impact resonance test. KSCE J Civil Eng 1997;1(1):11–8.
[19] Voigt T, Grosse C, Sun Z, Shah S, Reinhardt H. Comparison of ultrasonic wave transmission and reflection measurements with P- and S-waves on early age mortar and concrete. Mater Struct 2005;38(8):729–38.
[20] Valic MI. Hydration of cementitious materials by pulse echo USWR: Method, apparatus and application examples. Cem Concr Res 2000;30(10):1633–40.
[21] Voigt T, Shah SP. Properties of early-age portland cement mortar monitored with shear wave reflection method. ACI Mater J 2004;101(6):473–82.
[22] Kamada T, Uchida S, Rokugo K. Nondestructive evaluation of setting and hardening of cement paste based on ultrasonic propagation characteristics. J Adv Concr Technol 2005;3:343–53.
[23] Subramaniam K, Lee J. Ultrasonic assessment of early-age changes in the material properties of cementitious materials. Mater Struct 2007;40(3):301–9.
[24] Reinhardt HW, Grosse CU. Continuous monitoring of setting and hardening of mortar and concrete. Construct Build Mater 2004;18(3):145–54.
[25] Subramaniam KV, Wang X. An investigation of microstructure evolution in cement paste through setting using ultrasonic and rheological measurements. Cem Concr Res 2010;40(1):33–44.
[26] Zhang J, Weissinger EA, Peethamparan S, Scherer GW. Early hydration and setting of oil well cement. Cem Concr Res 2010;40(7):1023–33.
[27] Lee HK, Lee KM, Kim YH, Yim H, Bae DB. Ultrasonic in-situ monitoring of setting process of high-performance concrete. Cem Concr Res 2004;34(4):631–40.
[28] Trtnik G, Valic MI, Kavcic F, Turk G. Comparison between two ultrasonic methods in their ability to monitor the setting process of cement pastes. Cem Concr Res 2009;39(10):876–82.
[29] Trtnik G, Turk G, Kavcic F, Bosiljkov VB. Possibilities of using the ultrasonic wave transmission method to estimate initial setting time of cement paste. Cem Concr Res 2008;38(11):1336–42.
[30] Boumiz A, Vernet C, Tenoudji FC. Mechanical properties of cement pastes and mortars at early ages: evolution with time and degree of hydration. Adv Cem Mater 1996;3(3–4):94–106.
[31] Azenha M, Magalhães F, Faria R, Cunha Á. Measurement of concrete *E*-modulus evolution since casting: a novel method based on ambient vibration. Cem Concr Res 2010;40(7):1096–105.
[32] Azenha M, Faria R, Magalhães F, Ramos L, Cunha Á. Measurement of *E*-modulus of cement pastes and mortars since casting, using a vibration based techinique. Mater Struct 2011;9:1–12.
[33] Maia L, Azenha M, Faria R, Figueiras J. Influence of the cementitious paste composition on the *E*-modulus and heat of hydration evolutions. Cem Concr Res 2011;41(8):799–807.
[34] P-Gd Gennes. On a relation between percolation theory and the elasticity of gels. Le Journal de physique – Lettres 1976;37:L1–2.
[35] Magalhães F, Cunha Á, Caetano E. Dynamic monitoring of a long span arch bridge. Eng Struct 2008;30(11):3034–44.
[36] Magalhães F, Cunha Á, Caetano E. Online automatic identification of the modal parameters of a long span arch bridge. Mech Syst Signal Process 2009;23(2):316–29.
[37] Welch P. The use of fast Fourier transform for the estimation of power spectra: a method based on time averaging over shortmodified periodograms. IEEE Trans Audio Electro-Acoust 1967;15(2).
[38] Chopra AK. Dynamics of structures theory and applications to earthquake engineering. Englewood Cliffs: Prentice Hall International; 1995.
[39] Bentz DP, Garboczi EJ. Percolation of phases in a three-dimensional cement paste microstructural model. Cem Concr Res 1991;21(2–3):325–44.
[40] Gauthier-Manuel B, Guyon E. Critical elasticity of polyacrylamide above its gel point. Journal de physique – Lettres 1980;41. L503-L5.
[41] Wadsö L. An experimental comparison between isothermal calorimetry, semi-adiabatic calorimetry and solution calorimetry for the study of cement hydration NORDTEST report TR 5222003.
[42] EN 197–1:2000 – Cement – Part 1: Composition, specifications and conformity criteria for common cements, 2000.
[43] Sant G, Ferraris CF, Weiss J. Rheological properties of cement pastes: a discussion of structure formation and mechanical property development. Cem Concr Res 2008;38(11):1286–96.
[44] Lothenbach B, Le Saout G, Gallucci E, Scrivener K. Influence of limestone on the hydration of Portland cements. Cem Concr Res 2008;38(6):848–60.
[45] Poppe A-M, De Schutter G. Cement hydration in the presence of high filler contents. Cem Concr Res 2005;35(12):2290–9.
[46] Frías M, de Rojas MIS, Cabrera J. The effect that the pozzolanic reaction of metakaolin has on the heat evolution in metakaolin-cement mortars. Cem Concr Res 2000;30(2):209–16.
[47] Langan BW, Weng K, Ward MA. Effect of silica fume and fly ash on heat of hydration of Portland cement. Cem Concr Res 2002;32(7):1045–51.
[48] Robeyst N, Grosse CU, De Belie N. Measuring the change in ultrasonic p-wave energy transmitted in fresh mortar with additives to monitor the setting. Cem Concr Res 2009;39(10):868–75.
[49] Kadri E-H, Duval R. Hydration heat kinetics of concrete with silica fume. Construct Build Mater 2009;23(11):3388–92.
[50] Snelson DG, Wild S, O'Farrell M. Heat of hydration of Portland Cement-Metakaolin-Fly ash (PC-MK-PFA) blends. Cem Concr Res 2008;38(6):832–40.